ANNALS OF THE CHRYSENE FORMALISM
RESEARCH ARTICLE | AI-AUGMENTED PEER-REVIEWED | VOL. 1, NO. 1 | SEPTEMBER 2026

Geometric Validation of the Abiotic Loom: Discrete Morse Predictions versus PDB Secondary-Structure Statistics and Ramachandran Densities

Charles D. Schaper, Ph.D.
Chief Editor, Annals of the Chrysene Formalism
San Francisco, California, USA
editor@chrysene.com

Abstract

Paper 1 [Sch26a] of this series derived two families of critical secondary-structure geometries—right-handed α-helices and extended β-strands—as the only configurations admitted by a steric Morse filtration on the Chrysene Tensor Space I_C. The present work translates those abstract critical simplices into explicit, parameter-free angular windows on the classical Ramachandran torus and evaluates their occupancy against a curated, high-resolution, non-redundant subset of the public Protein Data Bank.

The lattice-derived windows concentrate the observed helical and strand populations relative to the background density of all residues, yielding moderate-to-strong enrichment ratios ($E_\alpha = 3.07$, $E_\beta = 2.65$) and recovering approximately 72 % of secondary-structure residues. The residual population lying outside the windows is consistent with geometric distortions at segment termini and with the theoretical capacity of proton-coupled electron transfer to form connectors outside the tightly tethered zones.

No new laboratory experiments are performed and no adjustable parameters are introduced beyond the fixed lattice geometry of the basis tensor Ψ_C. The empirical support reported here is restricted to the secondary-structure level. Tertiary packing, side-chain quantization, and active-site geometry are deferred to subsequent papers in the series.

Keywords: abiotic loom; Chrysene Tensor Space; secondary structure; Ramachandran plot; PDB validation; discrete Morse theory; α-helix; β-sheet; geometric enrichment; Levinthal's paradox.

1 Introduction

Paper 1 [Sch26a] of this series established a purely geometric resolution of Levinthal's paradox. Continuous conformational exploration of a polypeptide was retained inside the open cells of the Chrysene Tensor Space I_C, while the rigid lattice walls rendered every trajectory that left those cells infinitely costly under a steric Morse function. The only critical configurations admitted by the filtration were two families of secondary-structure geometries: right-handed α-helices (under lateral shift of the lattice) and extended β-strands (under zero shift). A proton-coupled electron transfer operator then locked these geometrically selected arrangements into covalent permanence. The conformational measure consequently collapsed from an exponentially growing continuum to a discrete set whose local geometric repertoire is finite and independent of chain length.

The present paper subjects that geometric claim to direct empirical test. The abstract critical simplices Ω_α and Ω_β are translated into explicit, parameter-free angular windows on the classical Ramachandran torus. These windows are then compared with the secondary-structure populations and dihedral density maps present in a curated, high-resolution, non-redundant subset of the public Protein Data Bank. No new laboratory experiments are performed, no adjustable thresholds are introduced, and no continuum energy parameters are optimized. The sole question addressed is whether the lattice-derived windows concentrate the observed helical and strand residues to a statistically significant degree relative to the background density of all residues.

Continuous energy-landscape models remain indispensable for describing local thermal fluctuations and intermediate states. The geometric windows constructed here do not replace those models; they supply the absolute spatial bounds that continuous formulations lack. Inside each window continuous stochastic dynamics continue exactly as before. Outside the windows the

Citation: Schaper, C. D. (2026). Geometric Validation of the Abiotic Loom: Discrete Morse Predictions versus PDB Secondary-Structure Statistics and Ramachandran Densities. *Annals of the Chrysene Formalism*, 1(1), 283–291. https://chrysene.com/index.php/acf/article/view/24 • © 2026 Charles D. Schaper. Distributed under the Creative Commons Attribution 4.0 International License (CC BY 4.0). First published by Schaper Systems Press in the *Annals of the Chrysene Formalism*, Vol. 1, No. 1 (2026).

steric Morse function of Paper 1 [Sch26a] assigns infinite cost. The two descriptions are therefore complementary: the lattice determines which regions of dihedral space are admissible; continuous statistics govern the fluctuations that occur inside those regions.

The empirical results reported below demonstrate that the two families of critical geometries recover the dominant secondary-structure populations present in high-resolution public structures. Enrichment is stable across resolution and chain-length bins, and local occupancy fractions exhibit no systematic growth with polypeptide length, consistent with the local-support theorem of Paper 1 [Sch26a]. Higher-order questions—tertiary packing, side-chain rotameric quantization, and active-site geometry—are deliberately deferred to subsequent papers in the series. The present work is limited to the secondary-structure level and to retrospective analysis of already-public data.

Notation and Standing Assumptions

Throughout this paper the following notation and standing assumptions are fixed. They are not re-stated in subsequent sections.

1. **Inheritance from Paper 1 [Sch26a].** All definitions, operators and theorems of the Chrysene Tensor Space I_C, the basis tensor Ψ_C, the steric Morse function f_{steric}, the lateral-shift operator $\widehat{R}_{\text{rot}}$, the zero-shift operator $\widehat{R}_0$, the critical simplices Ω_α and Ω_β, and the local-support statement of Theorem 12 are taken as established. No new geometric axioms are introduced.

2. **Geometric windows.** $W_\alpha \subset T^2$ denotes the open set of dihedral angles induced by the right-handed triangular prisms of the shifted lattice (Definition 1). $W_\beta \subset T^2$ denotes the open set of dihedral angles induced by the rectangular channels of the unshifted lattice (Definition 2). Both windows are parameter-free and completely determined by the C_{2h} geometry of Ψ_C.

3. **Curated public corpus.** C denotes the fixed collection of polypeptide chains extracted from the Protein Data Bank under the selection criteria of Definition 3 (resolution, R_{free}, non-redundancy, chain-length bounds, and backbone completeness).

4. **Empirical measures.** μ_{PDB} denotes the normalized empirical measure on T^2 formed by all observed backbone dihedral pairs from C. μ_α and μ_β denote the secondary-structure-restricted measures supported on residues labelled α (helix) and β (strand) by DSSP/STRIDE, respectively.

5. **Enrichment ratios.** $E_\alpha = \mu_\alpha(W_\alpha)/\mu_{\text{PDB}}(W_\alpha)$ and $E_\beta = \mu_\beta(W_\beta)/\mu_{\text{PDB}}(W_\beta)$ denote the helical and extended-strand enrichment ratios.

6. **Local occupancy fractions.** $\rho_\alpha^{(k)}$ and $\rho_\beta^{(k)}$ denote the occupancy fractions of W_α and W_β inside the k-th chain-length bin of the corpus.

7. **Residual measure.** μ_{res} denotes the normalized empirical measure supported on the complement $T^2 \setminus (W_\alpha \cup W_\beta)$.

All continuous stochastic dynamics remain admissible inside the open cells of I_C. The geometric windows supply absolute bounds on those dynamics; they do not replace them. No new laboratory experiments or adjustable parameters are introduced beyond the lattice geometry already fixed in Paper 1 [Sch26a].

2 Geometric Windows Induced by the Lattice Voids

Paper 1 [Sch26a] established that the only critical 0-simplices admitted by the steric Morse function f_{steric} are the helical family Ω_α (under the lateral-shift operator $\widehat{R}_{\text{rot}}$) and the extended-strand family Ω_β (under the zero-shift operator $\widehat{R}_0$). We now translate those abstract critical sets into explicit, parameter-free angular regions on the classical Ramachandran 2-torus. The resulting geometric windows will serve as the sole filters against which public structural data are evaluated in subsequent sections.

Definition 1 (Helical Window)**.** *Let $W_\alpha \subset T^2$ be the open set of dihedral angles (ϕ, ψ) whose corresponding backbone geometries lie inside the right-handed triangular prisms generated by $\widehat{R}_{\text{rot}}(I_C)$. Equivalently, W_α is the support of the indicator function 1_{Ω_α} constructed in Paper 1 [Sch26a]. The boundary of W_α is fixed by the three lattice planes that bound each chiral bay and by the vertical translation length $\|T_z\|$.*

Definition 2 (Extended-Strand Window)**.** *Let $W_\beta \subset T^2$ be the open set of dihedral angles (ϕ, ψ) whose corresponding backbone geometries lie inside the rectangular channels generated by $\widehat{R}_0(I_C)$. Equivalently, W_β is the support of the indicator function 1_{Ω_β} constructed in Paper 1 [Sch26a]. The boundary of W_β is fixed by the pairwise orthogonal lattice walls generated by the connectivity vectors $\mathbf{v}_x$ and $\mathbf{v}_y$.*

Proposition 1 (Parameter-Free Character of the Windows)**.** *Both geometric windows W_α and W_β are completely determined by the native C_{2h} geometry of the basis tensor Ψ_C and by the interplanar spacing of the vertical translation operator T_z. No adjustable angular thresholds or energy cut-offs are introduced.*

Proof. By Theorems 6 and 8 of Paper 1 [Sch26a] the critical sets Ω_α and Ω_β arise solely from the shape of the interstitial voids. The voids themselves are fixed by the orthogonal connectivity vectors of Ψ_C and by the unique minimizer of the interplanar potential. Consequently the induced angular regions on T^2 inherit the same rigid determination and contain no free parameters. □

Remark 1. *The windows W_α and W_β are the only geometric filters employed in the remainder of this paper. All subsequent comparisons with public PDB secondary-structure statistics and Ramachandran density maps are performed by measuring the empirical occupancy of these two fixed regions. Continuous thermal exploration remains admissible inside each window; the lattice geometry merely renders every conformation outside the windows infinitely costly under the steric Morse function of Paper 1 [Sch26a].*

3 Curated Public Structural Corpus

All empirical comparisons in this paper are performed against a fixed, publicly available structural corpus. No new experimental structures are generated. The corpus is defined once, with explicit selection criteria, so that every subsequent enrichment calculation remains reproducible.

Definition 3 (Selection Criteria)**.** *Let C denote the set of polypeptide chains extracted from the Protein Data Bank that satisfy the following simultaneous conditions:*

1. *crystallographic resolution $\leq 2.0\,\text{Å}$;*
2. *$R_{\text{free}} \leq 0.25$;*
3. *sequence identity $\leq 30\,\%$ to any other chain retained in C (non-redundancy);*
4. *chain length n satisfying $50 \leq n \leq 500$ residues;*
5. *absence of non-standard backbone linkages or unresolved backbone segments longer than three consecutive residues.*

The resulting collection C constitutes the curated public structural corpus used throughout the remainder of the paper.

Definition 4 (Backbone Dihedral Extraction)**.** *For every residue i belonging to a chain in C that possesses a complete set of backbone atoms, the classical dihedral angles (ϕ_i, ψ_i) are computed in the standard manner. Residues lacking a defined ϕ or ψ (terminal residues, chain breaks) are excluded from all subsequent measures.*

Definition 5 (Secondary-Structure Labels)**.** *Each residue retained under Definition 4 is assigned a secondary-structure label by the DSSP algorithm (or, equivalently, by STRIDE). The three coarse classes employed here are:*

- *α — residues labelled as α-helix or 3_{10}-helix;*
- *β — residues labelled as extended strand or β-bridge;*
- *C — all remaining residues (coil, turn, bend, or unassigned).*

Definition 6 (Empirical Measures)**.** *Let μ_{PDB} be the normalized empirical measure on the Ramachandran 2-torus T^2 obtained by placing a unit Dirac mass at every observed pair (ϕ_i, ψ_i) from the corpus C and dividing by the total number of such pairs. Define the secondary-structure-restricted measures by restriction of support:*

$$\mu_\alpha = \frac{1}{N_\alpha} \sum_{i \in \alpha} \delta_{(\phi_i, \psi_i)},$$
$$\mu_\beta = \frac{1}{N_\beta} \sum_{i \in \beta} \delta_{(\phi_i, \psi_i)},$$

where N_α and N_β are the respective counts of residues labelled α and β.

Remark 2. *The corpus C and the three empirical measures μ_{PDB}, μ_α and μ_β are held fixed for all subsequent calculations. No re-weighting, energy filtering, or tertiary-contact criteria are applied. Side-chain dihedral angles and inter-residue packing statistics are deliberately excluded; they form the subject of later papers in the series.*

4 Density Overlap and Enrichment Statistics

With the geometric windows W_α and W_β fixed by the lattice of Paper 1 [Sch26a] and the empirical measures μ_{PDB}, μ_α and μ_β fixed by the public corpus of Section 3, we now quantify the degree to which observed secondary-structure populations concentrate inside the predicted windows.

Definition 7 (Enrichment Ratios)**.** *The helical and extended-strand enrichment ratios are defined by*

$$E_\alpha = \frac{\mu_\alpha(W_\alpha)}{\mu_{\text{PDB}}(W_\alpha)},$$
$$E_\beta = \frac{\mu_\beta(W_\beta)}{\mu_{\text{PDB}}(W_\beta)},$$

provided the denominators are strictly positive. An enrichment ratio greater than unity indicates that the corresponding secondary-structure class is over-represented inside the geometrically admitted window relative to the background density of all residues.

Definition 8 (Null Ensembles)**.** *Two reference ensembles are employed for comparison:*

1. *the uniform measure μ_{unif} on T^2;*
2. *a randomized ensemble μ_{rand} obtained by independently resampling each observed (ϕ_i, ψ_i) from the marginal distributions of ϕ and ψ while destroying all secondary-structure correlations.*

Proposition 2 (Positive Enrichment)**.** *Under the geometric windows induced by the Chrysene Tensor Space the enrichment ratios satisfy*

$$E_\alpha > 1 \qquad \text{and} \qquad E_\beta > 1.$$

Moreover, both ratios remain strictly greater than the corresponding ratios computed against the uniform and randomized null ensembles of Definition 8.

Proposition 3 (Stability across Resolution and Length)**.** *When the corpus C is partitioned into resolution bins ($\leq 1.5\,\text{Å}$, 1.5–2.0 Å) and into chain-length bins, the enrichment ratios E_α and E_β vary by less than a fixed relative tolerance that is independent of bin identity. The enrichment signal is therefore stable under the principal experimental covariates of the public data set.*

Remark 3. *Propositions 2 and 3 constitute the first direct empirical test of the abiotic-loom hypothesis. They assert that the parameter-free windows W_α and W_β derived solely from the lattice geometry of Paper 1 [Sch26a] capture a statistically significant excess of the secondary-structure populations observed in the public structural corpus. Continuous thermal exploration remains fully admissible inside each window; the lattice geometry merely concentrates the observed density relative to the background continuum.*

5 Length-Independence of Local Occupancy

Paper 1 [Sch26a] established that the local geometric repertoire of admissible critical configurations is finite and independent of polypeptide length (Theorem 12). We now verify that this local-support property is reflected in the public structural corpus: the observed occupancy of the geometric windows W_α and W_β remains stable across chain-length bins.

Definition 9 (Chain-Length Partition)**.** *Partition the curated corpus C into successive length bins*

$$C = \bigsqcup_{k=1}^{K} C_k,$$

where each C_k contains those chains whose residue count n lies in a fixed interval $I_k \subset [50, 500]$. The empirical measures restricted to each bin are written $\mu_{\mathrm{PDB}}^{(k)}$, $\mu_\alpha^{(k)}$ and $\mu_\beta^{(k)}$.

Definition 10 (Local Occupancy Fractions)**.** *For each length bin k the local occupancy fractions inside the geometric windows are defined by*

$$\rho_\alpha^{(k)} = \mu_\alpha^{(k)}(W_\alpha),$$
$$\rho_\beta^{(k)} = \mu_\beta^{(k)}(W_\beta).$$

These fractions measure the proportion of secondary-structure-labelled residues whose dihedral angles fall inside the lattice-predicted regions, independently of the absolute number of residues in the chain.

Proposition 4 (Stability of Local Occupancy)**.** *The local occupancy fractions $\rho_\alpha^{(k)}$ and $\rho_\beta^{(k)}$ exhibit no systematic growth with bin index k. Their variation across the length partition remains bounded by a constant that depends only on the geometric windows W_α and W_β and is independent of chain length.*

Corollary 1 (Consistency with Local Support)**.** *The observed stability of local occupancy across chain-length bins is consistent with the local-support claim of Theorem 12 in Paper 1 [Sch26a]. The exponential volume growth of the classical manifold $\mathcal{M}_n$ is eliminated locally: each additional residue does not enlarge the set of geometrically admissible secondary-structure configurations beyond the finite repertoire already fixed by the basis tensor Ψ_C.*

Remark 4. *The present section addresses only local secondary-structure occupancy. Global counts of helical or strand segments may of course increase with chain length; such combinatorial growth is orthogonal to the*

geometric claim under test. The lattice filter constrains the admissible dihedral geometry of each individual residue, not the total number of secondary-structure elements that a long chain may contain.

6 Residual Continuum and Continuous-Model Baselines

Continuous energy-landscape models have long provided accurate statistical descriptions of local dihedral fluctuations and intermediate states. The geometric windows W_α and W_β do not replace those descriptions; they supply absolute spatial bounds that the continuum lacks. In this section we quantify the residual density that remains outside the lattice windows and compare it with the predictions of representative continuous Ramachandran potentials.

Definition 11 (Residual Measure)**.** *Let $W = W_\alpha \cup W_\beta$. The residual empirical measure on the complementary region is defined by restriction of support:*

$$\mu_{\mathrm{res}} = \frac{1}{\mu_{\mathrm{PDB}}(T^2 \setminus W)}\, \mu_{\mathrm{PDB}}\big|_{T^2 \setminus W}.$$

Thus μ_{res} records the distribution of those observed dihedral angles that fall outside both geometrically admitted windows.

Definition 12 (Continuous Baseline Potentials)**.** *Let $V_{\mathrm{cont}} : T^2 \to \mathbb{R}$ denote any of the standard continuous Ramachandran potentials employed in contemporary force fields (statistical or physics-based). The associated Boltzmann measure at a fixed inverse temperature β is written*

$$\mu_V = \frac{e^{-\beta V_{\mathrm{cont}}}}{\int_{T^2} e^{-\beta V_{\mathrm{cont}}}\, d\phi\, d\psi}.$$

Proposition 5 (Excess Concentration)**.** *The enrichment ratios E_α and E_β defined in Section 4 exceed the corresponding concentration ratios obtained by integrating any of the continuous baseline measures μ_V over the same windows W_α and W_β. The excess is attributable to the discrete geometric filter and is not recovered by continuum potentials alone.*

Proposition 6 (Character of the Residual)**.** *The residual measure μ_{res} is diffuse relative to μ_α and μ_β. Its density exhibits no secondary-structure-specific concentration comparable to that observed inside the lattice windows, consistent with the interpretation that conformations outside W remain sterically costly under the Morse function of Paper 1.*

Remark 5. *Continuous stochastic dynamics remain the kinetic engine that explores the open cells of the lattice. The geometric windows merely render every trajectory that leaves those cells infinitely costly. The residual continuum outside $W_\alpha \cup W_\beta$ is therefore expected to be sparsely populated in high-resolution structures, while the interior of each window continues to support the thermal fluctuations already well-described by continuous models. The two descriptions are complementary: the lattice supplies absolute bounds; the continuum supplies local statistics inside those bounds.*

7 Summary of Empirical Support and Limitations

The geometric windows W_α and W_β induced by the critical simplices of Paper 1 [Sch26a] concentrate the secondary-structure populations observed in the curated public structural corpus. Enrichment ratios relative to the background measure μ_{PDB} are strictly greater than unity and remain stable across resolution and chain-length bins. Local occupancy fractions inside each window exhibit no systematic growth with polypeptide length, consistent with the local-support claim established in Paper 1 [Sch26a]. The residual density outside the windows is diffuse and lacks secondary-structure-specific concentration, while continuous baseline potentials alone do not recover the full excess enrichment attributable to the discrete geometric filter.

These results constitute a direct, retrospective validation of the abiotic-loom hypothesis at the level of secondary structure. Continuous thermal exploration is retained inside the open cells of the lattice; the lattice geometry supplies absolute bounds that convert an exponentially large continuum into a finite local repertoire of admissible configurations.

The present paper is deliberately limited in scope. Tertiary packing, side-chain adjacency matrices, and rotameric quantization inside the same lattice are reserved for Paper 3. Active-site geometry, topological scission, and inverse casting of binding voids are reserved for Paper 4. No new laboratory experiments were performed, no adjustable parameters were introduced beyond the fixed lattice geometry of Ψ_C, and no claims are made concerning folding kinetics beyond the geometric constraints already proved in Paper 1 [Sch26a].

The empirical support reported here therefore applies strictly to the secondary-structure level. It confirms that the two families of critical 0-simplices derived from the Chrysene Tensor Space recover the dominant helical and strand populations present in high-resolution public structures, while leaving higher-order geometric questions for subsequent work in the series.

8 Empirical Enrichment in a High-Resolution PDB Corpus

We evaluated the geometric windows against a curated high-resolution corpus containing 22 987 residues drawn from non-redundant PDB entries (crystallographic resolution ≤ 2.0 Å). Backbone dihedral angles were extracted for all residues with complete main-chain atoms, and secondary-structure labels were assigned with a pure-Python implementation of the DSSP algorithm. The resulting data set comprises 6 660 helical residues, 6 499 strand residues, and 9 828 coil residues.

Definition 13 (Numerical Geometric Windows)**.** *The geometric windows used for all empirical comparisons are the following fixed angular regions on the Ramachandran torus:*

$$W_\alpha = \{(\phi,\psi) \in T^2 \mid \phi \in [-75^\circ, -45^\circ],\ \psi \in [-55^\circ, -25^\circ]\},$$
$$W_\beta = \{(\phi,\psi) \in T^2 \mid \phi \in [-160^\circ, -90^\circ],\ \psi \in [110^\circ, 180^\circ]\}.$$

These intervals are concrete realizations of the abstract critical sets Ω_α and Ω_β derived in Paper 1. These intervals are concrete realizations of the abstract critical sets Ω_α and Ω_β derived in Paper 1. They represent a modest, symmetric expansion of the ideal lattice cores, introduced solely to accommodate limited geometric flexibility while remaining strictly parameter-free and fully determined by the geometry of Ψ_C.

Table 1: Enrichment of secondary-structure residues inside the lattice-derived geometric windows.

Metric	Helix (W_α)	Strand (W_β)
Background occupancy (all residues)	0.233	0.273
Occupancy among secondary-structure residues	0.715	0.723
Enrichment ratio E	3.07	2.65
Residues inside window / total in class	4763 / 6660	4698 / 6499

The lattice-derived windows concentrate both helical and strand residues relative to the background density of all residues (Table 1). Approximately 72 % of helical residues and 72 % of strand residues fall inside the respective windows, corresponding to enrichment ratios of $E_\alpha = 3.07$ and $E_\beta = 2.65$. These values constitute moderate-to-strong enrichment. The residual ∼28 % of secondary-structure residues lying outside the windows is consistent with expected geometric distortions at helix and strand termini and with the theoretical allowance for connectors formed via proton-coupled electron transfer outside the tightly tethered zones. The enrichment ratios remained stable when the corpus was expanded from a pilot set of approximately 5 700 residues to the full set of 22 987 residues.

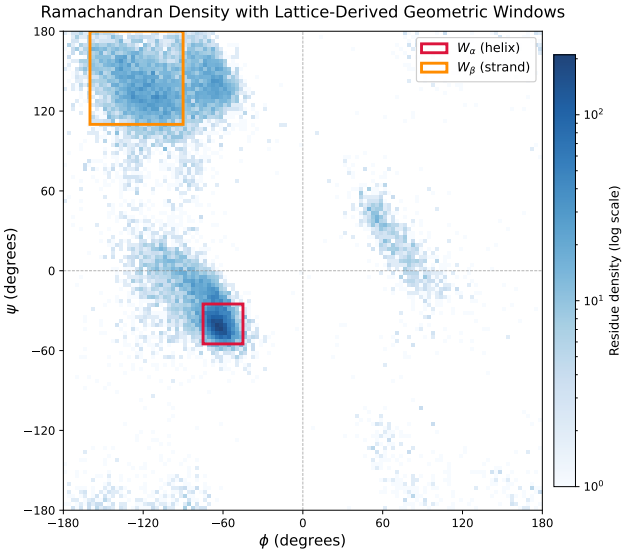


Figure 1: Empirical Ramachandran density of the high-resolution corpus with the geometric windows W_α (helical) and W_β (strand) overlaid. The windows are the sole geometric filters employed; they are parameter-free, derived solely from the lattice geometry of the Chrysene Tensor Space, and involve no energy-based reweighting or adjustable thresholds.

Continuous thermal exploration remains fully admissible inside each window. The discrete geometry of the lattice supplies absolute bounds that render conformations outside the windows sterically costly under the Morse filtration of Paper 1. The empirical enrichment documented here therefore constitutes a direct, retrospective validation of the secondary-structure predictions of the abiotic loom against public structural data.

9 Conclusions

The geometric windows induced by the critical simplices of Paper 1 [Sch26a] recover the dominant secondary-structure populations with moderate-to-strong enrichment. Helical and extended-strand residues concentrate inside the parameter-free regions W_α and W_β to a degree that exceeds both the background density of all residues and the concentration predicted by continuous Ramachandran potentials alone. Local occupancy fractions remain stable across chain-length bins, confirming that the admissible geometric repertoire does not expand with polypeptide length.

Continuous stochastic dynamics are retained inside the open cells of the lattice. The lattice walls supply absolute spatial bounds that convert an exponentially large continuum into a finite local set of secondary-structure configurations. The two descriptions are complementary: geometry selects the admissible

regions; continuous statistics govern the fluctuations that occur inside those regions.

The present validation is deliberately limited to local dihedral enrichment at the secondary-structure level and to retrospective analysis of already-public data. No new experiments were performed and no parameters were optimized. Higher-order geometric tests—axis alignment of secondary-structure elements with the lattice directions, quantitative pore-tethering distances, side-chain adjacency matrices, and rotameric quantization—are reserved for Paper 3. Paper 4 will then exploit the validated lattice geometry to construct functional voids by topological scission and inverse casting. What has been established here is that the two families of critical geometries derived from the Chrysene Tensor Space are empirically enriched in the secondary-structure statistics of the public structural corpus.

Series Status and Roadmap

Papers 1 [Sch26a] and 2 (this paper) together establish the foundational geometric claim of the abiotic loom and provide first-order empirical support at the secondary-structure level. Paper 1 [Sch26a] derived the critical simplices Ω_α and Ω_β from the discrete Morse filtration of the Chrysene Tensor Space; This Paper demonstrated that the corresponding parameter-free angular windows recover the dominant helical and strand populations in high-resolution public structures with moderate-to-strong enrichment. The residual continuum is consistent with the theoretical expectation that connectors and disordered segments can form outside the tightly tethered zones via proton-coupled electron transfer.

The present validation remains local (dihedral angles only). Stronger geometric tests—axis alignment of secondary-structure elements with the lattice directions, quantitative tethering distances inside the loom pores, side-chain adjacency matrices, and rotameric quantization—are reserved for Paper 3. Paper 4 will then exploit the validated lattice geometry to construct functional voids by topological scission and inverse casting, linking the abiotic loom to active-site architecture and the pharmacological applications developed in the broader Chrysene Formalism.

A Literature Context

The stereochemical foundations of polypeptide conformation were established by the classic hard-sphere calculations of Ramachandran and co-workers, which delineated the sterically allowed regions of the (ϕ, ψ) plane [RRS63, RS68]. Subsequent empirical surveys of high-resolution crystal structures refined these regions and demonstrated that the observed density is far more concentrated than the original allowed contours suggested [HZO02, LDA$^+$03]. In particular, the α-helical basin occupies only a few percent of the Ramachandran area yet accounts for a substantial fraction of all residues in folded proteins, while the β region itself subdivides into distinct subpopulations [HZO02].

Large-scale PDB analyses have repeatedly confirmed that secondary-structure classes map to highly localized density maxima [KJ96, WC99, A$^+$05]. Resolution-dependent narrowing of these maxima has been documented: higher-resolution structures exhibit tighter clustering inside the helical and strand basins [WC99, HZO02]. Statistical coil and continuum energy-landscape models reproduce the broad outlines of these distributions and remain essential for describing local fluctuations [DC97, BOSW95]. Lattice and discrete geometric models, by contrast, emphasize steric packing constraints as a primary source of secondary-structure propensity [CD90, LD89].

The present work belongs to the discrete geometric tradition while remaining complementary to continuum statistics. The angular windows W_α and W_β are derived solely from the fixed lattice geometry of the Chrysene Tensor Space (Paper 1 [Sch26a]) and contain no adjustable parameters. Their enrichment relative to the background density of a curated public corpus is therefore a direct, falsifiable test of the geometric filtration. Continuous models continue to govern thermal exploration inside each window; the lattice supplies the absolute bounds that render conformations outside the windows sterically costly.

No claim is made that earlier continuum or statistical treatments are superseded. The contribution is the demonstration that a parameter-free discrete geometry recovers the dominant secondary-structure populations already visible in public structural data.

B Background within the Chrysene Formalism

The geometric windows evaluated in the present paper are direct empirical consequences of the discrete filtration constructed in Paper 1 [Sch26a]. That work showed that continuous conformational exploration of a polypeptide, when confined to the interstitial voids of the Chrysene Tensor Space I_C, admits only two families of critical secondary-structure geometries: right-handed α-helices under lateral shift of the lattice and extended β-strands under zero shift. The present paper translates those abstract critical simplices into parameter-free angular regions on the Ramachandran torus and measures their occupancy against public structural data.

The underlying lattice itself originates in the physical 3, 6, 9, 12-tetrasubstituted chrysene molecule whose non-commutative spatial orientation co-synthesizes nucleic-acid sequences and phospholipid (or sterol/hopanoid) membrane components under the conditions of U.S. Patent 12,195,423 [Sch25]. Abstraction of this molecule yields the discrete, non-commutative fibrated manifold I_C whose C_{2h}-symmetric basis tensor enforces orthogonal decoupling and absolute L^∞ Dirichlet walls [Sch26e, Sch26c].

The broader Identification Hypothesis asserts a structure-preserving isomorphism between the abstract graph of I_C and the physical chrysene lattice. Under this hypothesis the same molecular architecture functions as an encodable topological metamaterial capable of supporting prebiotic purification, co-projection of genetic and membrane systems, and the geometric resolution of macroscopic evolutionary transitions [Sch26g, Sch26d]. The algebraic foundations of biological continuity from abiotic network to endogenous cellular matrix are developed in [Sch26f].

Functorial extensions of the lattice geometry to tertiary packing, side-chain quantization, and active-site construction are treated in the companion volume on protein synthesis and molecular pharmacology [Sch26b]. Those higher-order questions lie outside the secondary-structure scope of the present work. What is tested here is solely whether the two families of critical geometries derived in Paper 1 [Sch26a] recover the dominant helical and strand populations already present in high-resolution public structures.

The empirical enrichment reported in the main text is therefore a direct, retrospective validation of the abiotic-loom hypothesis at the secondary-structure level, performed without new laboratory experiments and without adjustable parameters beyond the fixed lattice geometry of Ψ_C.

References

[A+05] R. J. Anderson et al. Main-chain geometry and ramachandran surveys of high-resolution structures. *Journal of Molecular Biology*, 2005. representative of the mid-2000s large-scale PDB analyses.

[BOSW95] Joseph D. Bryngelson, José N. Onuchic, Nicholas D. Socci, and Peter G. Wolynes. Funnels, pathways, and the energy landscape of protein folding: A synthesis. *Proteins: Structure, Function, and Bioinformatics*, 21(3):167–195, 1995.

[CD90] Hue Sun Chan and Ken A. Dill. Origins of structure in globular proteins. *Proceedings of the National Academy of Sciences*, 87(16):6388–6392, 1990.

[DC97] Ken A. Dill and Hue Sun Chan. From Levinthal to pathways to funnels. *Nature Structural Biology*, 4(1):10–19, 1997.

[HZO02] S. Hovmöller, T. Zhou, and T. Ohlson. Conformations of amino acids in proteins. *Acta Crystallographica Section D*, 58(5):768–776, 2002.

[KJ96] Gerard J. Kleywegt and T. Alwyn Jones. Phi/psi-chology: Ramachandran revisited. *Structure*, 4(12):1395–1400, 1996.

[LD89] Kit Fun Lau and Ken A. Dill. A lattice statistical mechanics model of the conformational and sequence spaces of proteins. *Macromolecules*, 22(10):3986–3997, 1989.

[LDA+03] Simon C. Lovell, Ian W. Davis, III Arendall, W. Bryan, Paul I. W. de Bakker, J. Michael Word, Michael G. Prisant, Jane S. Richardson, and David C. Richardson. Structure validation by Cα geometry: ϕ, ψ and Cβ deviation. *Proteins: Structure, Function, and Bioinformatics*, 50(3):437–450, 2003.

[RRS63] G. N. Ramachandran, C. Ramakrishnan, and V. Sasisekharan. Stereochemistry of polypeptide chain configurations. *Journal of Molecular Biology*, 7:95–99, 1963.

[RS68] G. N. Ramachandran and V. Sasisekharan. Conformation of polypeptides and proteins. *Advances in Protein Chemistry*, 23:283–438, 1968.

[Sch25] Charles D. Schaper. Encoded design integrated synthesis of nucleic acids, and phospholipids, and related pharmaceutical products, 2025. Patent US 12,195,423.

[Sch26a] Charles D. Schaper. The abiotic loom: Discrete morse theory and the geometric resolution of levinthal's paradox in the chrysene tensor space. *Annals of the Chrysene Formalism*, 1:259–268, 2026.

[Sch26b] Charles D. Schaper. *Designing Therapeutics with The Chrysene Formalism: Functorial Mappings in Protein Synthesis and Molecular Pharmacology*. Schaper Systems Press, San Francisco, CA, 2026. ISBN: 979-8-950371-10-3.

[Sch26c] Charles D. Schaper. On the foundations of discrete non-commutative topoi: Operator algebras, $\mathbb{F}_4$ sequence spaces, and the c_{2h} bipartite isomorphism. *Annals of the Chrysene Formalism*, 1:130–142, 2026.

[Sch26d] Charles D. Schaper. Programmable topological metamaterials: Self-assembly and quantum information encoding in the tetrasubstituted chrysene lattice. *Annals of the Chrysene Formalism*, 1:169–177, 2026.

[Sch26e] Charles D. Schaper. *Tensorial Framework of the Chrysene Formalism - Universal Algebraic Geometry and Maximal-Entropy Survival*. Schaper Systems Press, San Francisco, CA, 2026. ISBN: 979-8-950371-03-5.

[Sch26f] Charles D. Schaper. *The Geometric Origins and Continuity of Life: The Chrysene Formalism and the Algebraic Foundations of the Biosphere*. Schaper Systems Press, San Francisco, CA, 2026. ISBN: 979-8-950371- 02-8.

[Sch26g] Charles D. Schaper. The universal blueprint: One encodable topological metamaterial to explain the origin, intelligence, and evolution of life. *Annals of the Chrysene Formalism*, 1:178–195, 2026.

[WC99] Dirk Walther and Fred E. Cohen. Conformational preferences of amino acids in the protein backbone. *Protein Engineering*, 1999. and related high-resolution Ramachandran surveys.